Fabrication of metallic multi-material components using Laser Metal Deposition

Frank Brueckner[1,3], Mirko Riede[1], Michael Mueller[1], Franz Marquardt[1,2], Matthias Knoll[1], Robin Willner[1,2] André Seidel[1,2], Elena Lopéz[1], Christoph Leyens[1,2], Eckhard Beyer[1,2]

[1] Fraunhofer Institute for Material and Beam Technology IWS Dresden
[2] Technische Universität Dresden
[3] Luleå University of Technology

Abstract

Meanwhile, Laser Metal Deposition (LMD) is a well-known Additive Manufacturing technology used in various industrial branches as energy, tooling or aerospace. It can be used for the fabrication of new components but also repair applications. So far, volume build-ups were mostly carried out with one single material only. However, loading conditions may strongly vary and, hence, the use of more than one material in a component would yield major benefits. By means of multi-material build-ups, cost-intensive alloys could be used in highly-loaded areas of the part, whereas the remaining part could be fabricated with cheaper compositions. The selection of combined materials strongly depends on the requested thermo-physical and mechanical properties. Within this contribution, possibilities of material combinations by LMD and selected examples of beneficial multi-material use are presented.

Introduction

In several industrial branches, Laser Metal Deposition (LMD) is already a common technology for coating applications, part refurbishment but also for manufacturing of functional components. Due the process' suitability to a broad spectrum of materials (e.g. Fe-, Ni-, Co- or Ti-based alloys) LMD is used for a large range of products such as components for jet engines, turbines, tooling or medical implants. The LMD is a nozzle based manufacturing process (see Figure 1). The powdery material is blown into the process zone by the nozzle. The laser-powder interaction causes a preheating of the powder particles. The preheated particles are then finally absorbed by the induced melt pool and deposited on the substrate.

Before being blown into the process zone by the nozzle, different powder materials can be mixed in-situ by an integrated powder-mixing chamber (see Fig. 1). Due to the possibility of a continuous as well as localized control of the mixing ratio, an in-situ alloying process without any additional joining can be achieved by LMD [1…5].

Material combinations such as Ti-Ta, Fe-Ta or Fe-Cu are highly interesting for industrial applications but cause several issues due to differing thermo-physical properties, poor miscibility or differing absorptivity. Therefore an in depth understanding of process conditions (temperature fields, stress gradients), material properties (micro- and macrostructure) and occurring failure mechanisms is obligatory for an industrial transfer. In order to counter these problems the following approaches for layer wise multi-material build-up by LMD with powder shall be investigated within this paper:

I.   sharp material transition of binary material combinations,
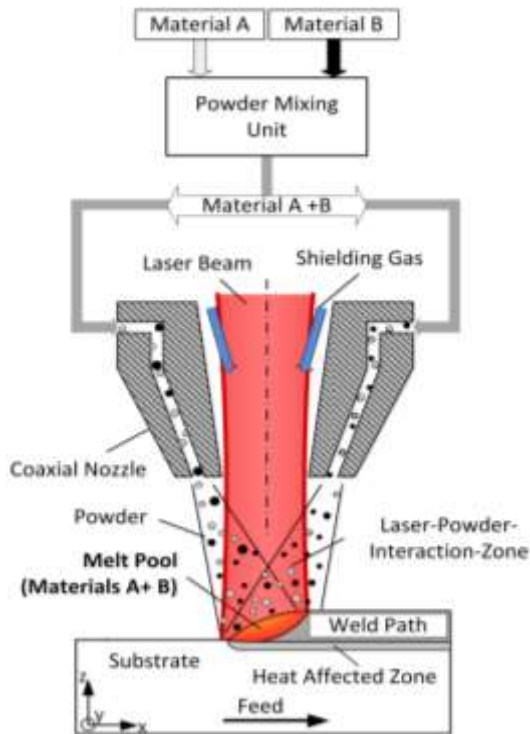II. graded material transition of binary material combinations.

Figure 1: Powder-based multi-material LMD processing [6]

I Sharp material transition of binary material combinations

Ti6Al4V – Ta: Ti6Al4V exhibits good mechanical properties as well as biocompatibility and is therefore a commonly used material for the fabrication of implants. Due to better osseiointegration properties and biocompatibility tantalum can be used for improving the integration of implants into the human body. Therefore combining tantalum and Ti6Al4V could lead to lightweight implants with good mechanical properties and an increased lifetime [7].

Nevertheless, joining Ti6Al4V and tantalum raises the issue of a large gap between the melting ranges of the materials (see Table 1). Due to the high melting temperature of tantalum the simultaneous processing of these materials may cause local evaporation phenomena, which may lead to the formation of pores. By using an active

cooling the Ti6Al4V substrate can be prevented from evaporation whilst fully melting the tantalum powder material. Furthermore since Ti6Al4V as well as tantalum are susceptible to oxidation at high temperatures processing has to be conducted using a shielding gas atmosphere.

Table 1: Mechanical and Thermo-physical properties of Ta and Ti6Al4V [8, 9]

	Ti6Al4V	Ta
Density [g/cm³]	4,45	16,6
Yield Strength [MPa]	828	170
CTE at 20 °C [10E-6/K]	8,9	6,5
Melting Range [°C]	1604-1660	2996
Evaporation Temperature [°C]	3260	5458

As can be seen in the binary phase diagram (see Figure 2) titanium and tantalum show good miscibility at low temperatures and there is no formation of intermetallic phases. Furthermore due to similar CTE the bonding zone is less susceptible to thermally induced cracking.
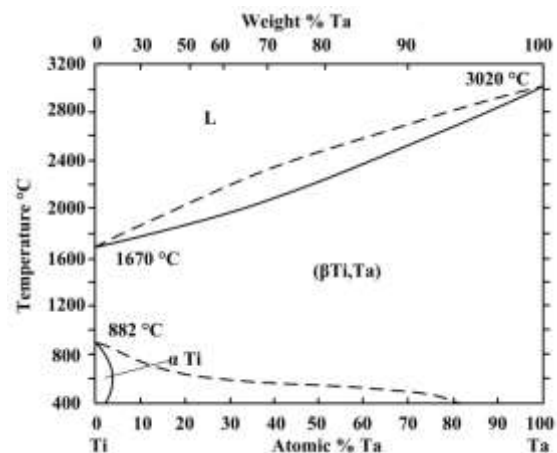

Figure 2: Ti-Ta binary phase diagram [10]

Taking into account the stated processing characteristics Ti6Al4V and tantalum were successfully joined by LMD. A transition from Ti6Al4V to tantalum without any cracks and almost no pores could be achieved (see Figure 3). The high processing

temperatures induced a large melt pool. Due to the large gap between the melting temperatures and convection phenomena within the melt pool partial solidification of high melting tantalum areas within a lower melting matrix can be observed (see Figure 3 and Figure 4)
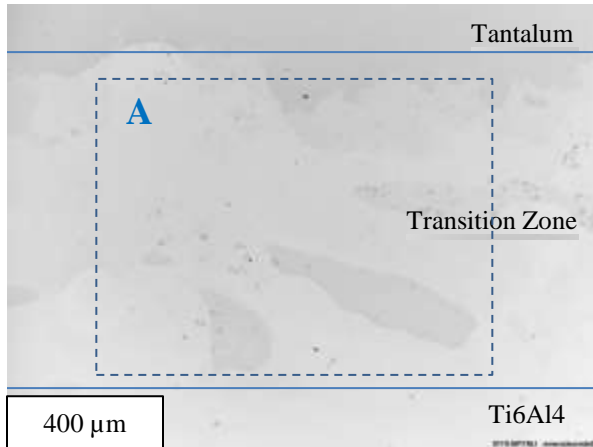

Figure 3: Metallographic image of the LMD transition zone from Ti6Al4V to Ta
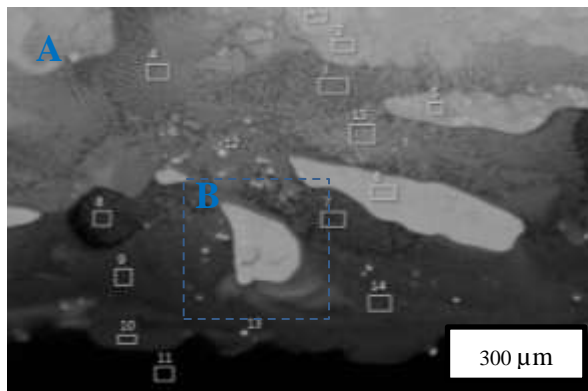

Figure 4: SEM Image of the LMD transition from Ti6Al4V to Ta; BSE analysis of marked region

A BSE analysis of the transition zone showed the formation of areas with a broad range of differing chemical compositions (see Figure 4 and Figure 5). A significant characteristic of the transition zone is the formation of two major phases. The tantalum content of first phase (see Figure 4 and Figure 5, spectrum 1, 5) is above 80 at. %. Additionally ßTi, Al, and V can be found within this phase. The microstructure of this

phase is homogenous, which could be a result of the short solidification time due to a small melting range. The second phase (see Figure 4 and Figure 5, spectrum 7, 11, 15) shows a tantalum content of less than 80 at. %. Moreover, this phase also consists of αTi, Al, V and exhibits a very fine dendritic microstructure. This microstructure might be caused by the increased solidification time due to a larger melting range. Furthermore, due to the high melting temperature (3020 °C) of pure tantalum small (diameter approx. 5 µm) globular pure tantalum areas we formed within a matrix with a higher content of Ti, Al and V (see Figure 6 and Figure 7, spectrum 19, 20).
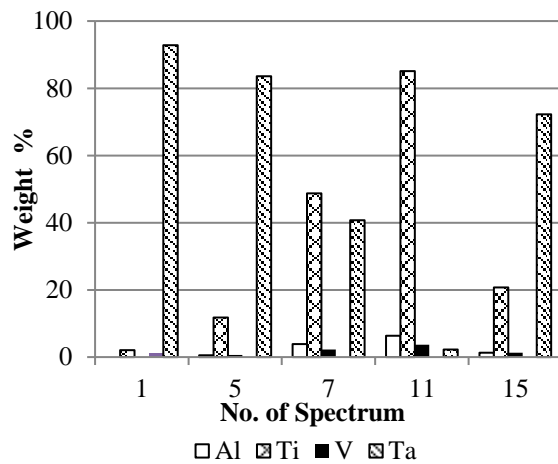

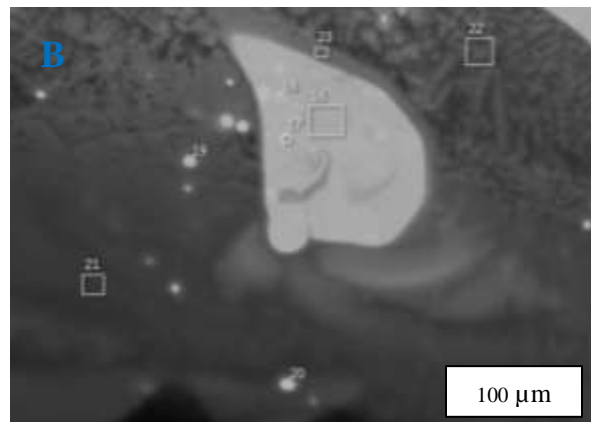**Figure 5: Results of BSE analysis of the investigated areas 1-15**

Figure 6: SEM Image of LMD Ti6Al4V/tantalum transition; BSE analysis of marked region
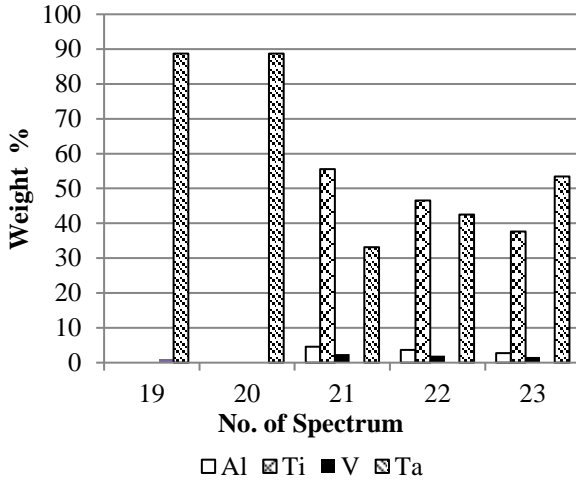
Figure 7: Results of BSE analysis of the investigated areas 16-23

Tantalum - SS AISI 316L: Besides the use for medical application due to the high melting temperature and excellent corrosion resistance tantalum is also highly attractive for applications in the chemical and energy industry. Since the procurement of tantalum is very expensive three dimensional multi-material processing of tantalum in combination with low cost corrosion resistant materials such as stainless steel could enable new cost efficient design and manufacturing possibilities.

In this paper, the deposition of SS 316L on commercially pure tantalum shall be presented. The multi material processing of tantalum and SS 316L raises three major issues. As stated above due to the high melting temperature of tantalum the simultaneous processing of tantalum and lower melting materials may cause local evaporation phenomena, which may lead to the formation of pores. Secondly tantalum and SS 316L show a significant difference in CTE. This may lead to thermally induced crack within the bonding zone. (see Table 2)

Furthermore, as can be seen in the binary Fe-Ta phase diagram in Figure 8, iron and tantalum only have a limited miscibility and tend to the formation of intermetallic

phases. Especially the Laves structure ε phase (Fe_2Ta) may cause an embrittlement of the bonding zone.

Table 2: Mechanical and Thermo-physical properties of Ta and SS 316L [10, 11]

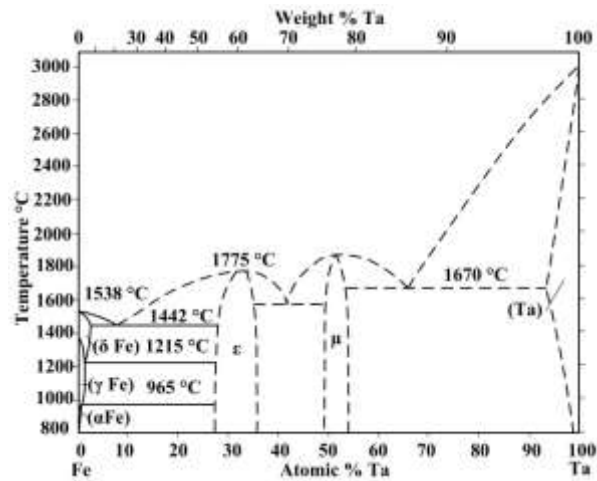|	SS 316L	Ta
Density [g/cm³]	7,99	16,6
UTS [MPa]	558	285
Yield Strength [MPa]	290	170
CTE at 20 °C [10E-6/K]	15,9	6,5
Melting Range [°C]	1304-1371	2996

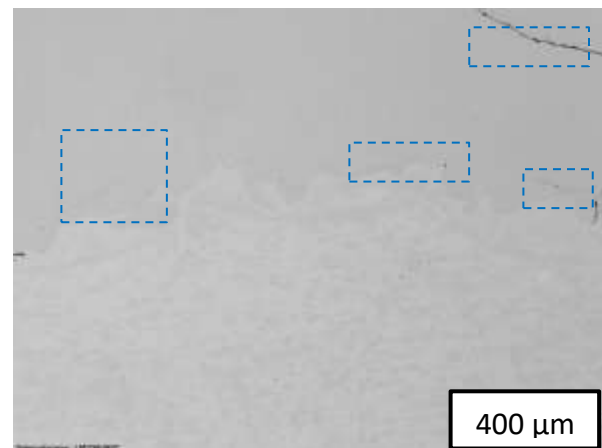**Figure 8: Binary Fe-Ta phase diagram [12]**

400 µm

Figure 9: Metallographic image of SS 316L deposited by LMD on tantalum substrate

For ensuring a full melting of the tantalum substrate the LMD process was

combined with simultaneous conduction heating of the substrate. The process parameters were optimized in order to ensure low evaporation of the SS 316L whilst fully melting the tantalum and in order to prevent the tantalum from oxidation at high temperatures.

As can be seen in Figure 9, a dense transition from tantalum to SS316 L and a high degree of fusion could be achieved. Nevertheless, as mentioned before, this material combination is very susceptible to thermally induced cracking due to differing thermal expansion. The highlighted areas in Figure 9 show the formation of micro cracks along the transition zone. Beside the large CTE difference the formation of intermetallics may be another reason for the formation of cracks. Figure 10 shows a very inhomogeneous material distribution within the transition zone, which indicates the presence of different metallic phases. In order to investigate the single phases BSE analysis shall be conducted.
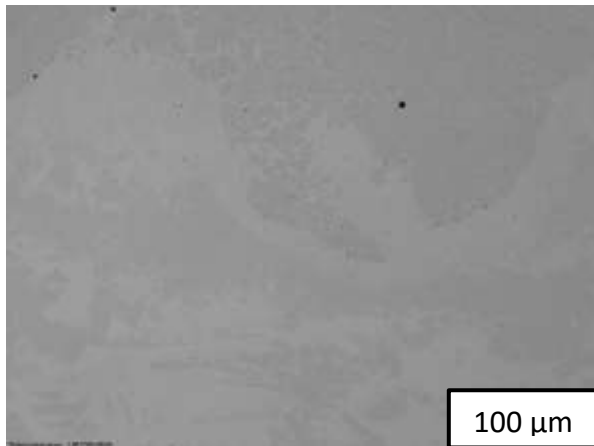

100 µm

Figure 10: Metallographic image of SS 316L deposited by LMD on tantalum substrate

AISI SS3 04L – Copper: Due to its excellent thermal and electrical conduction but poor mechanical properties, integrating copper into multi-material systems is highly relevant for industrial applications. Therefore joining stainless steel, which provides beneficial mechanical properties, and cooper shows high potential for industrial applications such as conductor tracks, heat exchangers or coatings on thermal-loaded parts [13].
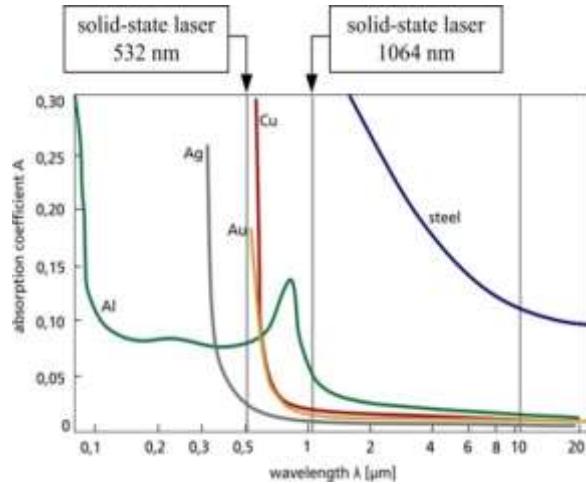

Figure 11: Wavelength dependence of the absorption rate of different metals

Joining copper to stainless steel causes two major issues: Due to the great difference in NIR absorptivity between copper (approx. 2 %) and stainless steel (approx. 50 %) a high level of power is required to overcome the low absorptivity of copper and to fully melt both materials (see Figure 11). Furthermore due to the increasing absorptivity at higher temperatures the sudden temperature jump while melting may lead to an overshooting and blow out of molten material. Therefore, a green laser source with a wavelength of 532 nm was used.

Secondly in Figure 12 can be seen that the binary copper-iron system shows limited miscibility with two peritectic points. One peritectic point is on the copper rich side at 1096 °C with 3.5 % miscibility of iron in copper. The second one is on the iron rich side at 1485 °C with a maximum miscibility of 7.5 % in γ-Fe.
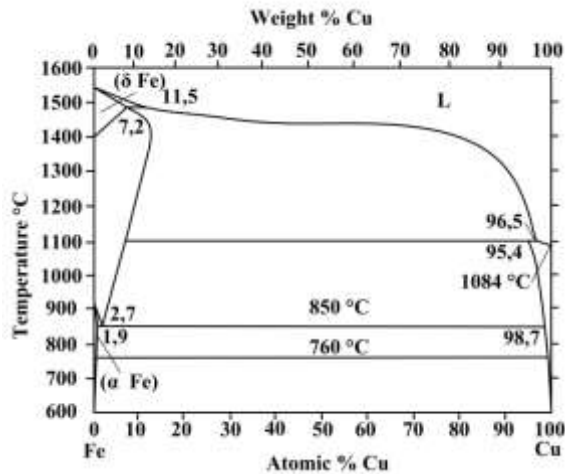
Figure 12: Fe-Cu binary phase diagram [14]

Figure 13: LMD copper track on SS 304 L

Figure 14: SEM of the copper track

The operating parameters were optimized in order to obtain non-porous volumes and low penetration of the filler material (see Figure 13). The microstructure of the single track is characterized by inhomogeneous distributed globules in a copper-rich matrix (see Figure 14 and Figure 15). By EDX analysis the composition of the copper track was determined. The copper-rich matrix exhibits a composition with 3.5 at. % Fe. This approves with the binary phase diagram in Figure 12. Once the melt pool temperature falls below the solidus temperature first regions with a higher amount of Fe start to solidify and form globular areas due to surface tension. Therefore the amount of Fe in the melt decreases until the peritectic point at 96.5 at. % Cu is reached. At this point the remaining melt solidifies and forms the matrix with peritectic composition. Due to decreasing miscibility of iron in copper with sinking temperature iron rich segregations are likely to occur at the grain borders. The uneven distribution of the globules within the matrix can be explained by the Marangoni-convection, which is driven by thermally and/or concentration induced surface tension gradients. The chemical composition of the globules is close to the iron-rich peritectic composition with 11 at. % Cu.
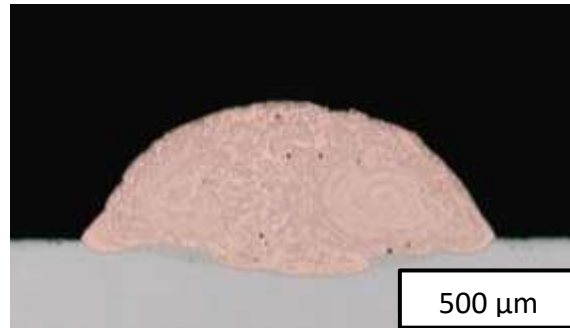

Figure 15: EDX spectrum of zones A and B of Figure
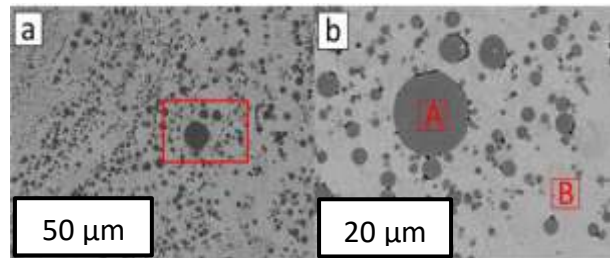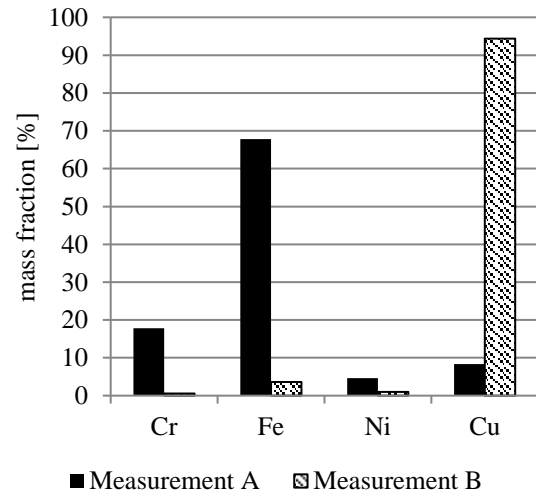
II Graded material transition of binary material combinations

SS AISI 316L – INCONEL 718: As already mentioned the joining of multi-materials may cause severe stresses within the transition zone due to differing thermos-physical and mechanical properties. Therefore a graded transition (see Figure 12) within the

bonding zone is a promising approach for decreasing stress gradients and reducing cracking. Within this work the graded transition from SS AISI 316L to the nickel-based superalloy INCONEL 718 shall be presented (see Figure 16 and Figure 17).
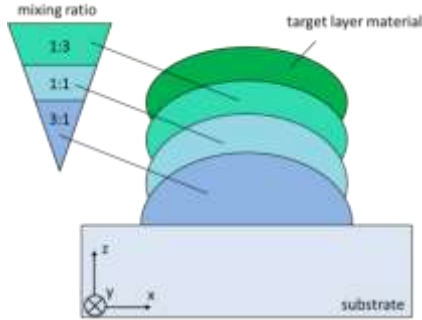

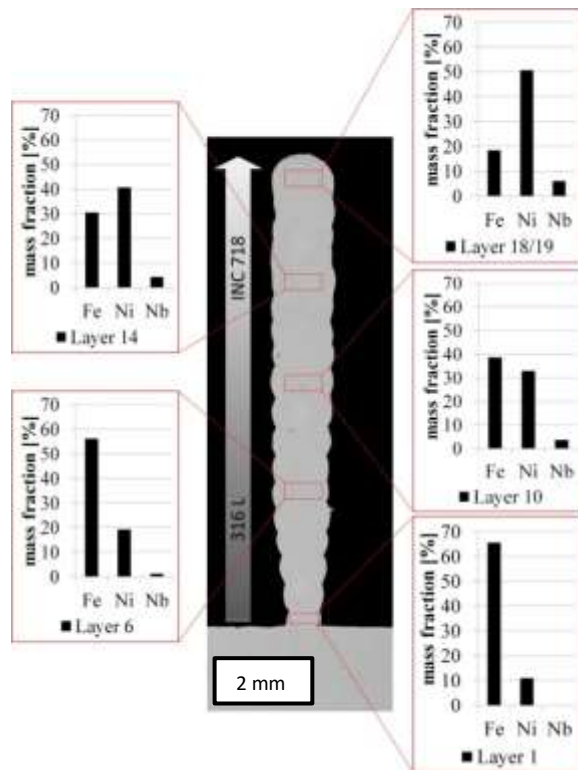**Figure 16: Functional principle of graded LMD transitions**

Figure 17: Metallographic image and EDX analysis (Fe, Ni, Nb) of the generated AISI 316L-INC718 graded material transition

Based on two layers of SS 316, deposited on a SS 304L substrate, the composition of the powder mixture used for

building up the transition was linearly varied in order to gradually replace the amount of SS 316L by INCONEL 718. The metallographic image in Figure 17 shows that a dense and almost crack free volume with only a little amount of pores was achieved. By EDX analysis the chemical transition process was investigated (see Figure 17). Since there is no Nb in SS 316L but approx. 5.0 weight % in INCONEL 718 Nb was used as a marker element for detecting the gradual transition.

The EDX analysis, which was conducted at the layers 1, 6, 10, 14 and 19 shows that in the bottom layer a crack free deposition of SS 316L was achieved. Starting in layer 3 the feeding rates were adapted linearly in order to accomplish a linear transition from SS 316L to INCONEL 718. The linear growth of the Nb mass fraction, which was measured by EDX, indicates a linear transition from SS 316L to INCONEL 718 (see Tab. 3). Furthermore, the EDX analysis of layer 19 confirms that the SS 316L has been fully replaced by Inconel 718.

Table 3: Chemical composition of the generated AISI 316L-Inconel 718 graded material transition (EDX)

Layer	Fe [%]	Ni [%]	Cr [%]	Mo [%]	Mn [%]	Nb [%]
Inconel 718	rest	50.0-55.0	17.0-21.0	2.8-3.3	0.35	4.7 - 5.5
19	18.4	50.6	19.7	3.8	0	6
14	30.6	40.7	19.5	3.3	0.4	4.4
10	38.7	32.9	19.3	3.6	0.7	3.6
6	56.1	19.2	18.8	3.1	1.1	1.2
1	65.5	11.0	18.9	2.6	1.4	0.0
SS 316L	rest	10.0-13.0	17.5-19.5	2.0-2.5	0.0-2.0	0.0

Nevertheless, the layer wise modification of the powder mixture composition also raises the issue of ensuring a homogenous material

distribution within each layer. An uneven material mass fraction distribution may cause an inhomogeneous microstructure and therefore differing thermo-physical and mechanical properties within a single layer.

The metallographic image in Figure 18 confirms that within a single layer different micro structures can be found. Figure 18 C shows a coarse columnar grain structure whereas Figure 18 A exhibits a fine and rather equiaxed grain structures. This indicates the in situ alloying of different metallic or intermetallic phases in dependence of the local mass fraction distribution. Moreover, according to Figure 18 B local micro cracking along the grain orientation has occurred. This may indicate a local embrittlement due to undesired local phase formation.
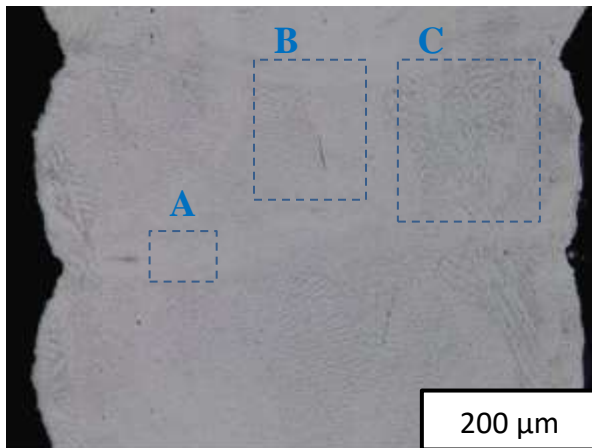

Fig. 18: Metallographic image of the generated SS 316L-INCONEL 718 material transition (layer 6)

Conclusion and Outlook

Within this paper, the three dimensional processing of multi-materials by Laser Metal Deposition, related benefits and resulting major issues are presented. Therefore this work gives an overview for LMD multi-material combinations with high industrial relevance. The following materials combinations were investigated:

- Ti6Al4V – Tantalum
- SS 316L – Tantalum
- SS 304L – CP Copper
- SS 316L – INCONEL718

Moreover the following processing approaches were applied:

- Sharp material transition of binary material combinations
- Graded material transition of binary material combinations

The investigations on LMD processing Ti6Al4V have shown that a dense, crack free material transition can be achieved. Due to the high melting temperature of tantalum a high degree of fusion could be observed. Furthermore the good miscibility at low temperatures and the high degree of fusion causes the formation of locally varying phases with differing microstructures.

The multi-material processing of SS 316L and tantalum clearly showed that by using substrate heating a dense transition with a sufficient degree of fusion can be accomplished. Nevertheless the major issues of differing CTE and formation of intermetallics caused micro cracking within the transition zone. Therefore different ways for avoiding these phenomena shall be investigated within further research.

The successful multi-material processing of the material combinations Ti6Al4V/Ta and SS 316L/Ta might be a promising approach for the dissimilar joining of Ti6Al4V and SS 316L using tantalum as interlayer material. This approach shall be investigated within further research.

Moreover an analysis of a SS 304L and CP copper transition zone manufactured by LMD was conducted. Due to poor miscibility and a high melting range the transition zone shows a composite structure consisting of iron rich globules within a cooper rich matrix. Due to the peritectic behaviour of the Fe-Cu material

system the matrix exhibits a Fe atomic fraction of 3.5 at. %. The globules characteristic distribution within the peritectic matrix may result from the occurring Marangoni effect.

The great number of different material combinations and, moreover, the broad range of industrial applications shows the high potential of the LMD process for multi-material fabrication. However, as can be seen in this paper, metallurgical incompatibility, undesired local in situ alloying phenomena and varying thermo-physical properties are still challenges for this manufacturing approach, which shall be overcome within future research.

Literature

[1] Yakovlev, A., Bertrand, P. u. Smurov, I.: Laser cladding of wear resistant metal matrix composite coatings. Thin Solid Films 453-454 (2004), S. 133–138

[2] Wu, X.: In situ formation by laser cladding of a TiC composite coating with a gradient distribution. Surface and Coatings Technology 115 (1999) 2-3, S. 111–115

[3] Shah, K., Haq, I. u., Khan, A., Shah, S. A., Khan, M. u. Pinkerton, A. J.: Parametric study of development of Inconel-steel functionally graded materials by laser direct metal deposition. Materials & Design (1980-2015) 54 (2014), S. 531–538

[4] Li, W., Yan, L., Karnati, S., Liou, F., Newkirk, J., Taminger, K. M. B. u. Seufzer, W. J.: Ti-Fe intermetallics analysis and control in joining titanium alloy and stainless steel by Laser Metal Deposition. Journal of Materials Processing Technology 242 (2017), S. 39–48

[5] Kotoban, D., Aramov, A. u. Tarasova, T.: Possibility of Multi-material Laser Cladding Fabrication of Nickel Alloy

and Stainless Steel. Physics Procedia 83 (2016), S. 634–646

[6] Brueckner, F.: Modellrechnungen zum Einfluss der Prozessführung beim induktiv unterstützten Laser-Pulver-Auftragschweißen auf die Entstehung von thermischen Spannungen, Rissen und Verzug. Stuttgart: Fraunhofer Verlag 2012

[7] Balla, V. K., Banerjee, S., Bose, S. u. Bandyopadhyay, A.: Direct laser processing of a tantalum coating on titanium for bone replacement structures. Acta biomaterialia 6 (2010) 6, S. 2329–2334

[8] Titan Grade 5 / Titane Grade 5, thyssenkrupp Materials Schweiz, 2017

[9] Mills, K. C.: Recommended Values of Thermophysical Properties for Commercial Alloys. Cambridge: Woodhead Pub 2002

[10] Das, K. u. Das, S.: A review of the Ti-Al-Ta (Titanium-Aluminum-Tantalum) system. Journal of Phase Equilibria and Diffusion 26 (2005) 4, S. 322–329

[11] 316/316L STAINLESS STEEL DATA SHEET, AK Steel Corporation, 2007

[12] Swartzendruber, L. J. u. Paul, E.: The Fe−Ta (Iron-Tantalum) system. Bulletin of Alloy Phase Diagrams 7 (1986) 3, S. 254–259

[13] EB industries: Copper to Stainless Steel Welding, 2017. https://www.ebindustries.com/CU_to_SST_Welding, abgerufen am: 16.05.2017

[14] Yao, C., Xu, B., Zhang, X., Huang, J., Fu, J. u. Wu, Y.: Interface microstructure and mechanical properties of laser welding copper–steel dissimilar joint. Optics and Lasers in Engineering 47 (2009) 7-8, S. 807–814